Fusing High Resolution, Physically-Based Models and Remote Sensing to Understand and Predict Water Fluxes and Stocks

Hernan A. Moreno, Ph.D.
Assistant Professor
School of Atmospheric and Geographic Sciences

11/15/2018

Research Associates

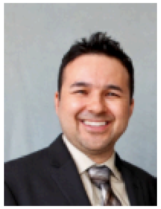

Hernan Moreno

Assistant Professor
Department of Geography and Environmental Sustainability
Google Scholar Profile

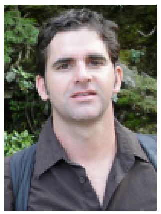

J.J. Gourley

Research Hydrologist
National Severe Storms Laboratory– NOAA
Google Scholar Profile

Hamed Zamani Sabzi

Postdoctoral Research Associate
Multi–critera optmization for watershed restoration. Modeling for watershed restoration and conservation.

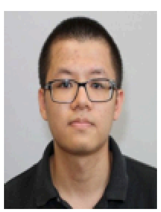

Tri Pham

MS student in Civil Engineering
Distributed hydrologic modeling of soil moisture and evapotranspiration.

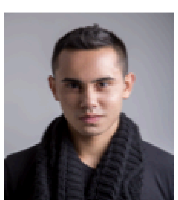

Jorge Celis

MS student in Geography
Distributed hydrologic Modeling. Surface Energy Budget and soil temperature profiles at eddy flux sites.

Laura Alvarez

Postdoctoral Research Associate
Center for Automated Sensing and Sampling
Google Scholar Profile

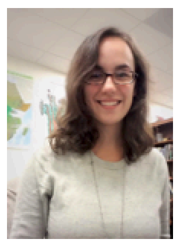

Rachel Fovarge

Postdoctoral Research Associate
Balancing water usage and ecosystem outcomes under drought and climate change through optimization modeling

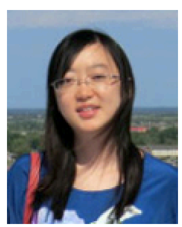

Zhen Hong

PhD student in Geography.
Remote sensing hydrology.Evaluation of satellite imagery and use for water resources planning.

SCIENCE TO SHAPE THE FUTURE OF THE ARMY
ARMY RESEARCH OFFICE
1951

Great Plains
Landscape Conservation Cooperative

USGS
science for a changing world

Outline

1. Improving hyper-resolution modeling for watershed predictions.
2. Hydrologic effects of forest disturbance
3. Real-time river flood forecasting
4. Soil moisture and ET processes
5. Bathymetry and surface water storage using smart sampling systems

tRIBS:
Tin-based Real-time Integrated Basin Simulator

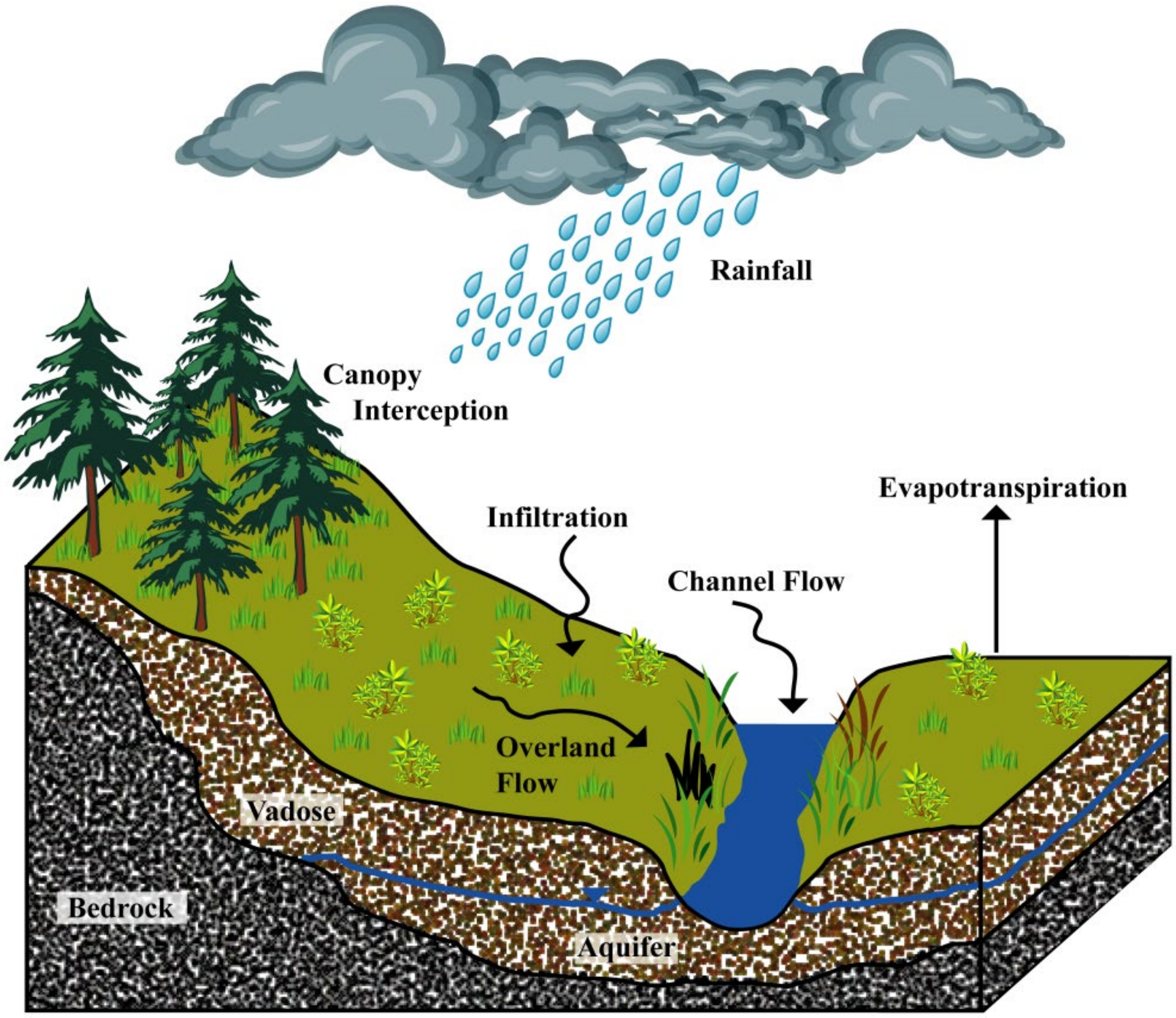

- Need for process-based modeling constantly remarked in journal opinion papers.
- Distributed and continuous.
- Topography, land cover and soils types.
- Coupled vadose and saturated zones.
- Runoff mechanisms and channel routing.
- Water and energy balance.
- Snow processes

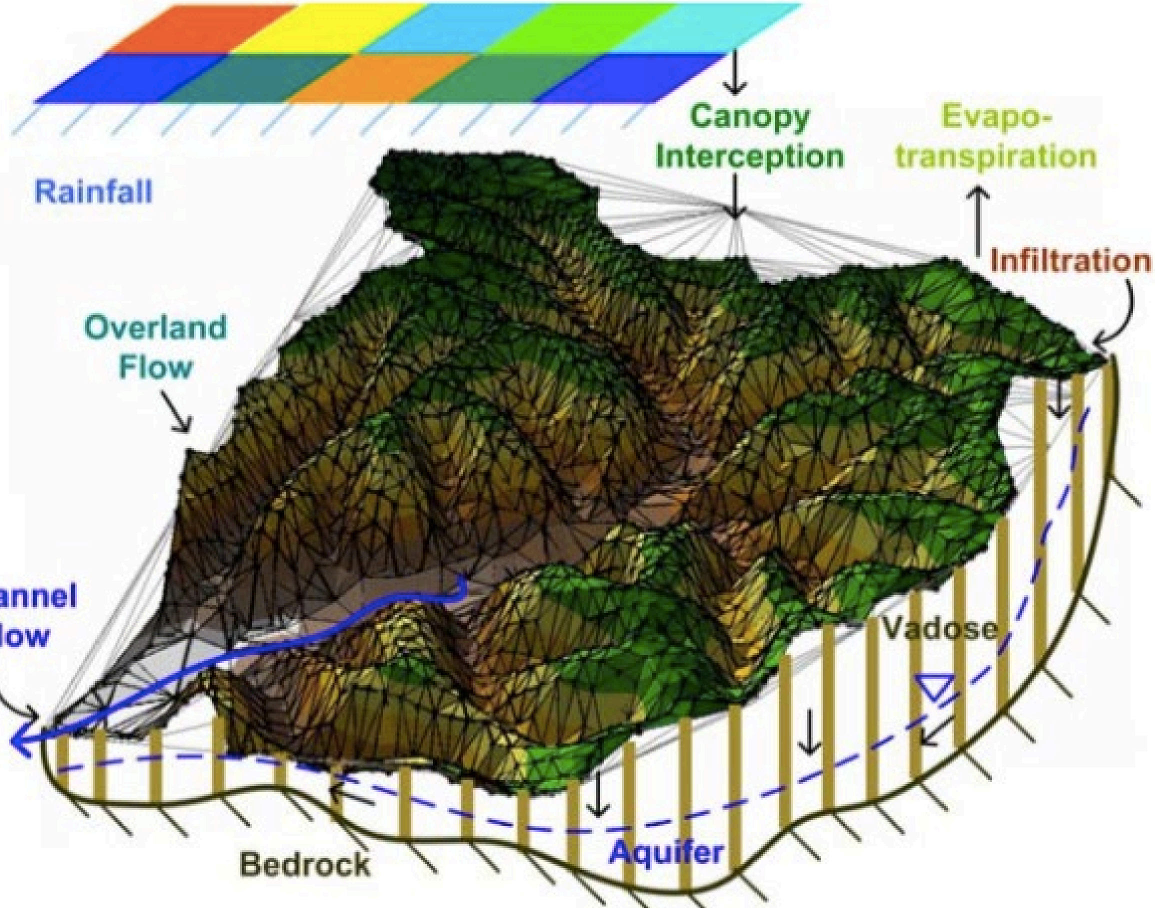

Table II. Hydrologic components of the tRIBS distributed hydrologic model

Model process	Description
Rainfall interception	Canopy water balance model
Surface energy balance	Combination equation (λE), gradient method (H) and force-restore equation (G)
Surface radiation model	Short-wave and long-wave components accounting for terrain variability
Evapotranspiration	Bare soil evaporation, transpiration and evaporation from wet canopy
Infiltration	Kinematic approximation with capillarity effects; unsaturated, saturated and perched conditions; top and wetting infiltration fronts
Lateral vadose flow	Topography-driven lateral unsaturated and saturated vadose flow
Runoff production	Infiltration-excess, saturation-excess, perched return flow and groundwater exfiltration
Groundwater flow	Two-dimensional flow in multiple directions, dynamic water table
Overland flow	Nonlinear hydrologic routing
Channel flow	Kinematic wave hydraulic routing

What are the spatially distributed hydrologic effects of forest thinning?

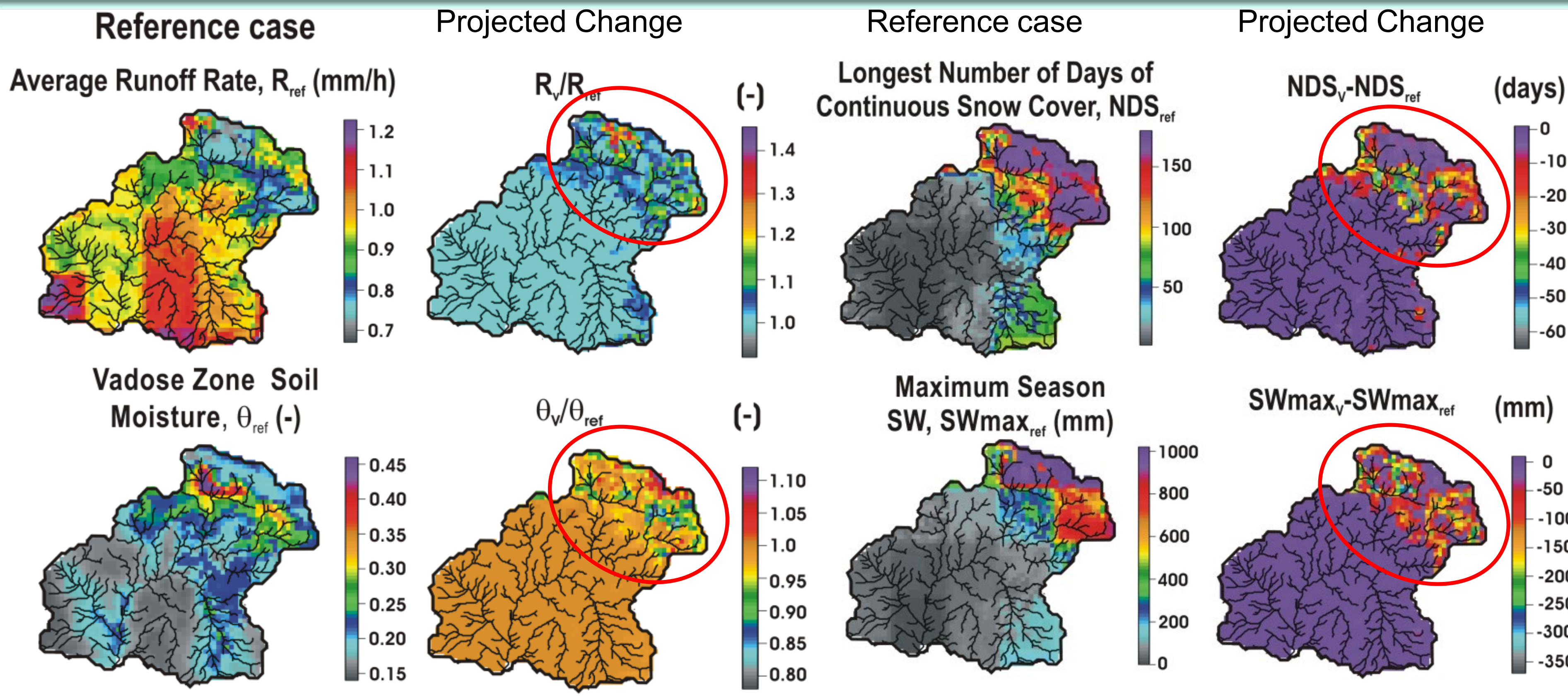

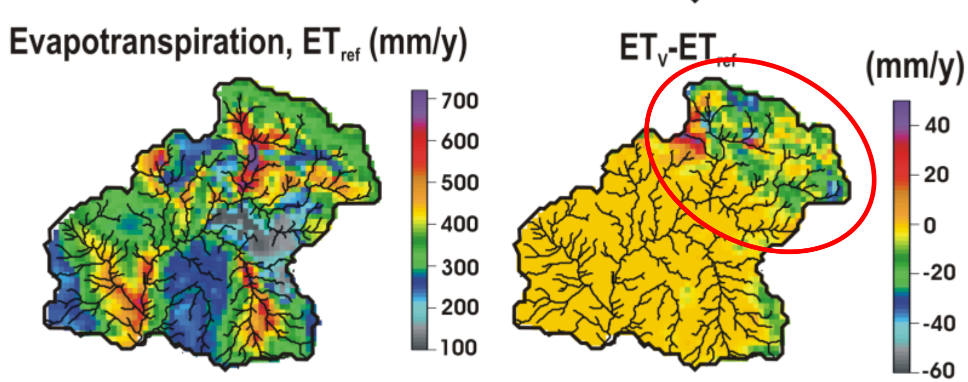

Local runoff increases

Soil moisture and ET mixed patterns

Days with snow cover reduced between 1 and 60 days

Max. snow water reduced in 350 mm

Participatory modeling for water security

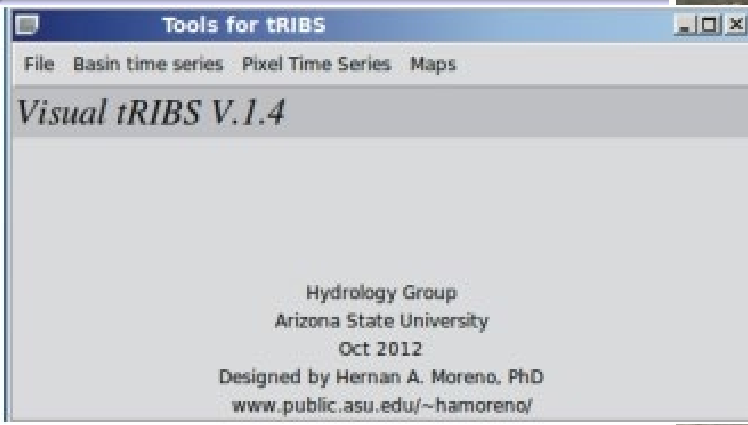

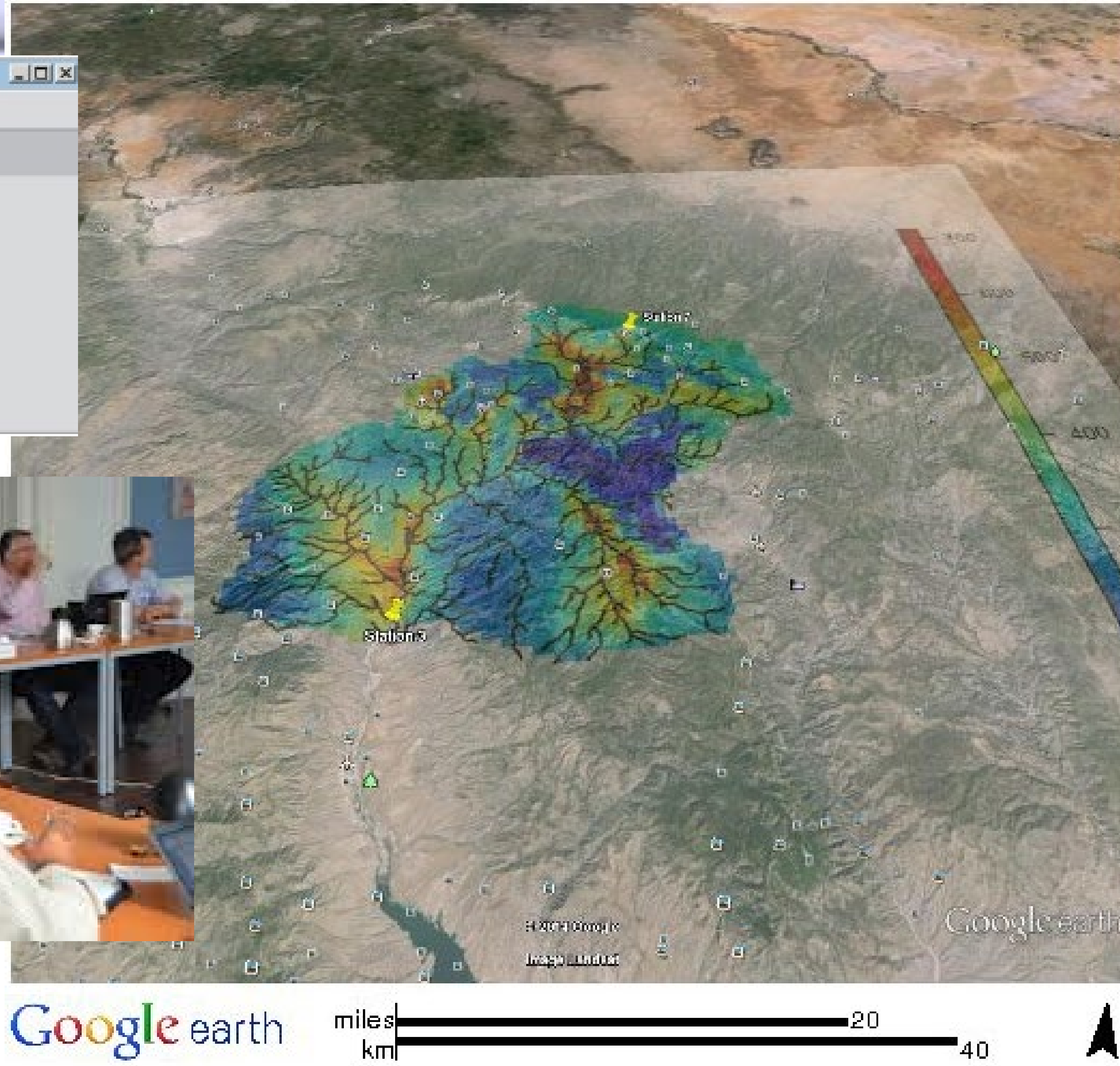

Radar nowcasts + tRIBS

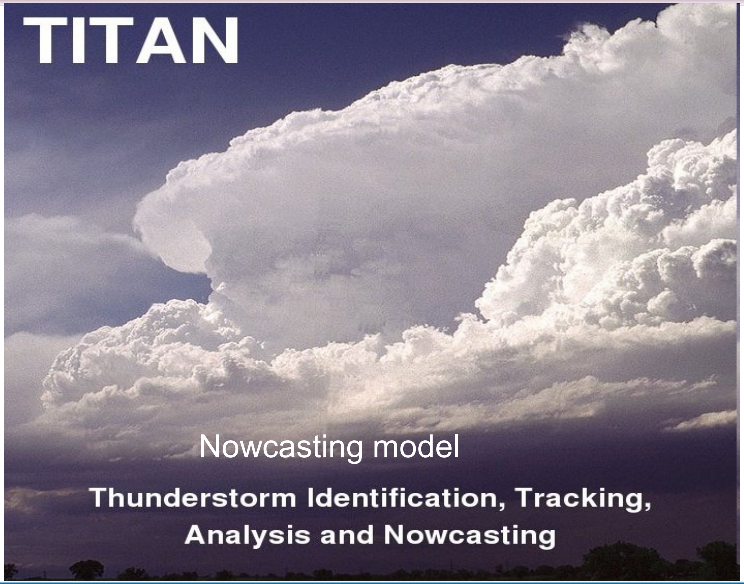

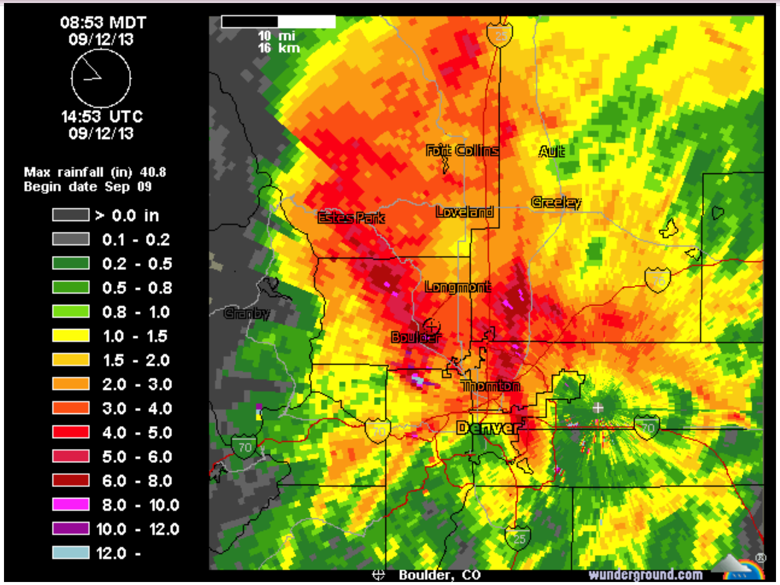

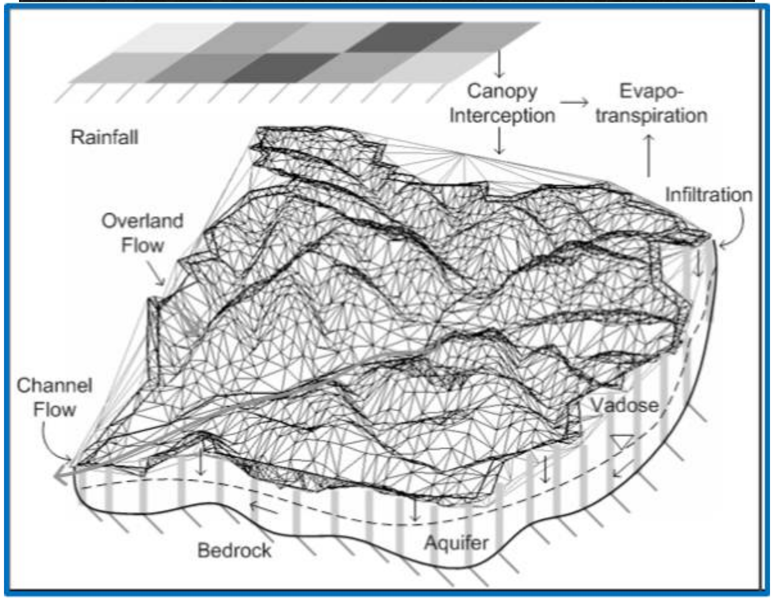

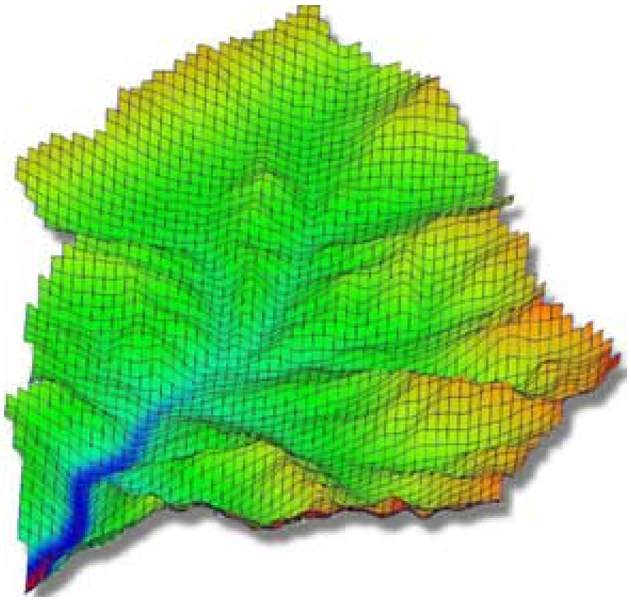

tRIBS: Tin-based Real Time Integrated Basin Simulator

What basin sizes are more predictable?

Standard Error

$$SE = \frac{Q_R}{A_c MA}$$

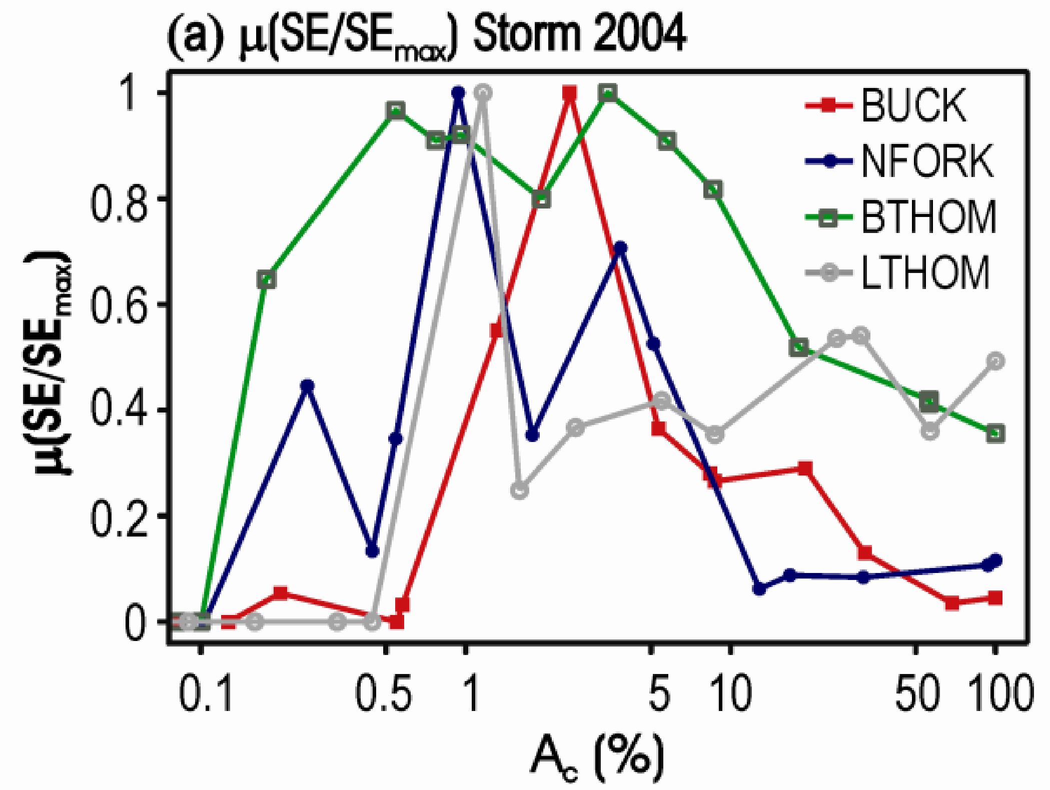

Floods less predictable at Intermediate size basins (1-10% of total Area) as a result of an increased fraction of runoff producing zones.

Virtual Mesonet Eddy-Covariance

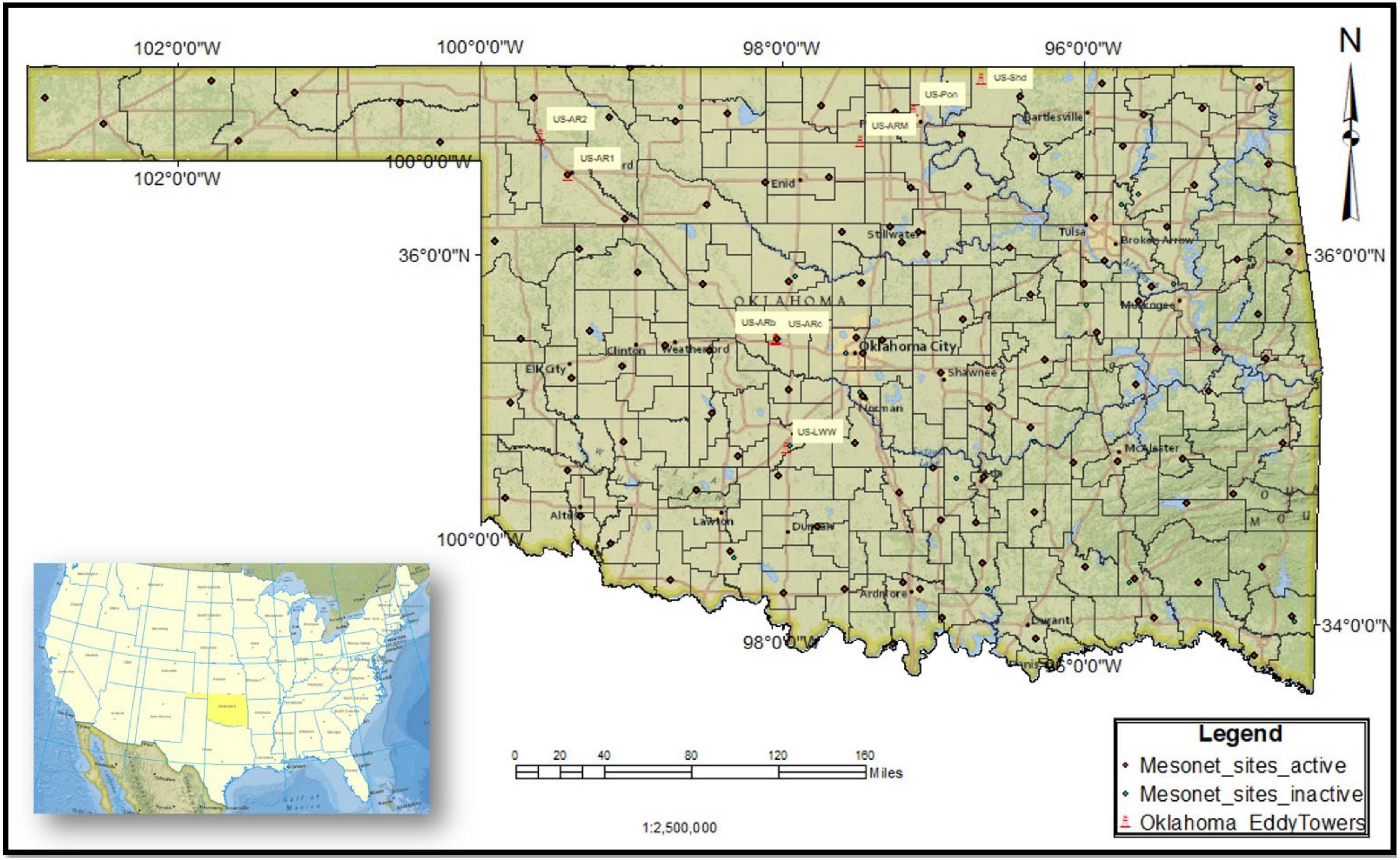

Preliminary simulations at one eddy station

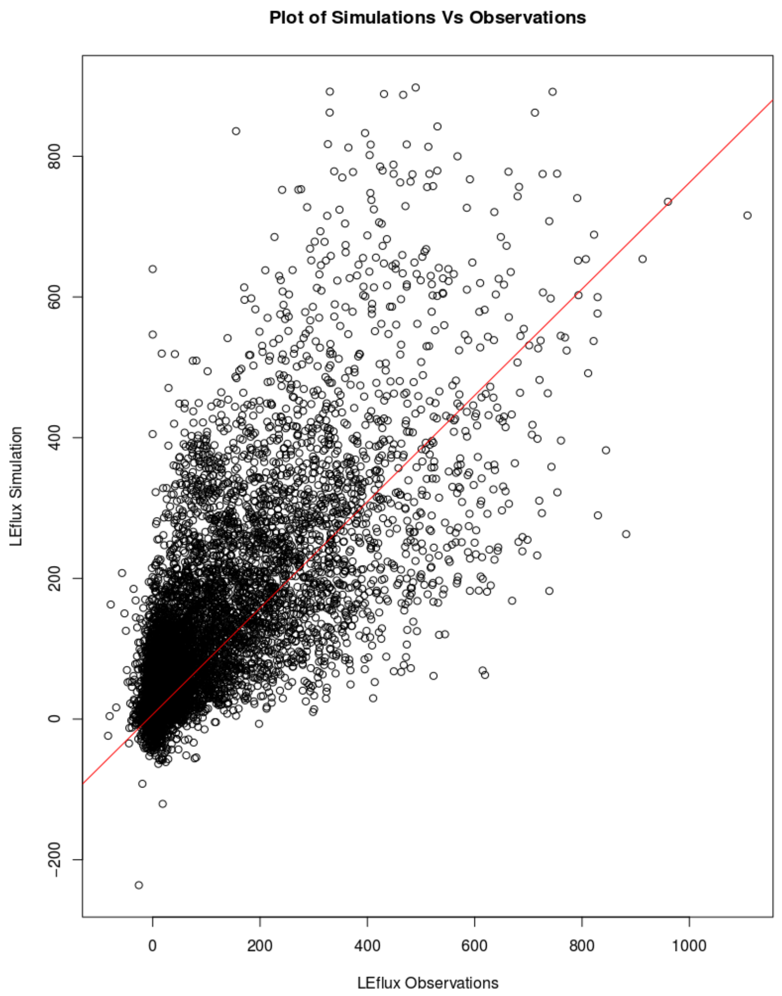

Latent heat flux

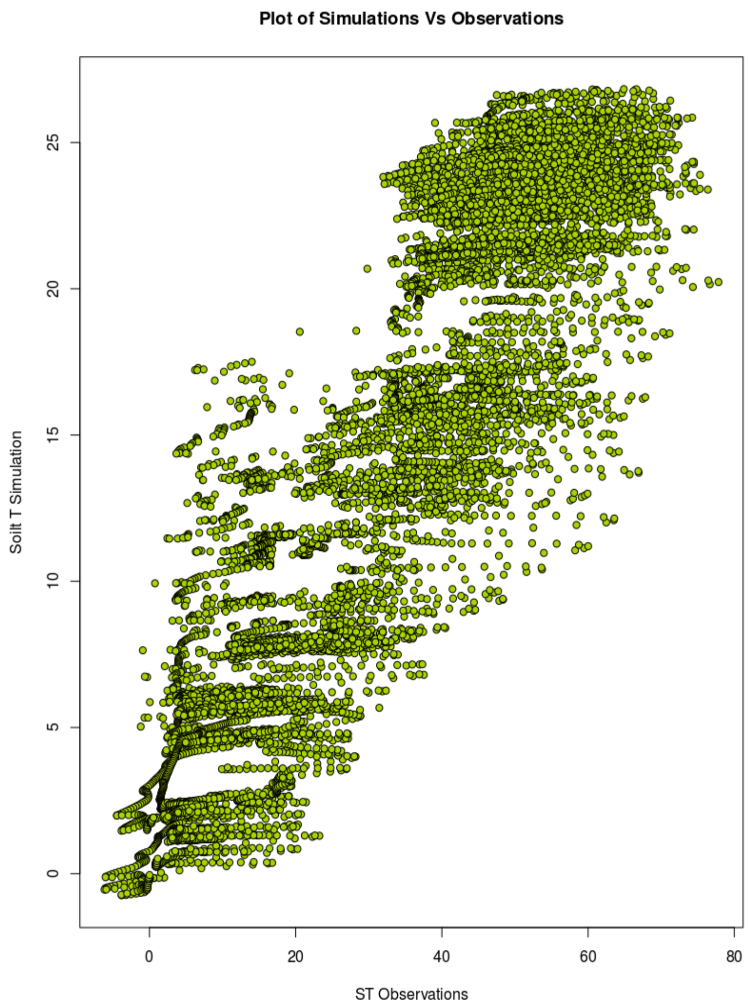

Soil surface temperature

Fusing L-band radiometers and observations to improve continuous and accurate modeling

Figure 4. Tempest UAS illustrating location of LDCR an[d] MiCo antenna elements.

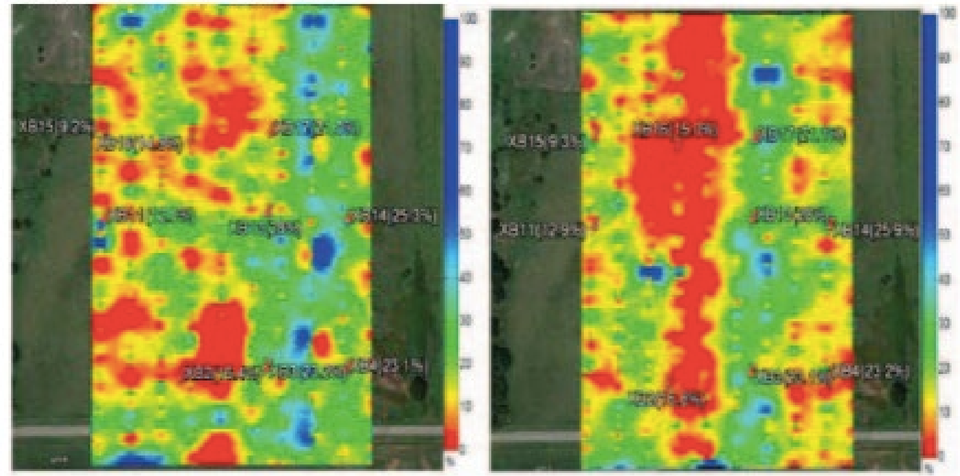

(a) (b)

Figure 5: Google earth images overlay of LDCR retrieved VSM maps and in-situ measured VSM, data from (a) September 8th, (b) September 9th.

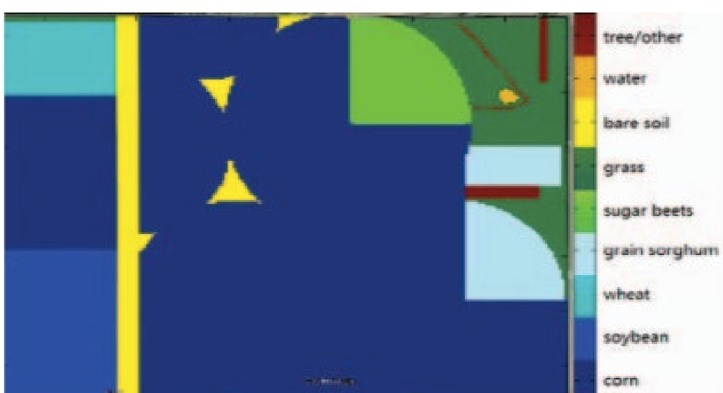

Figure 7: Land cover classification of IRF mapping area.

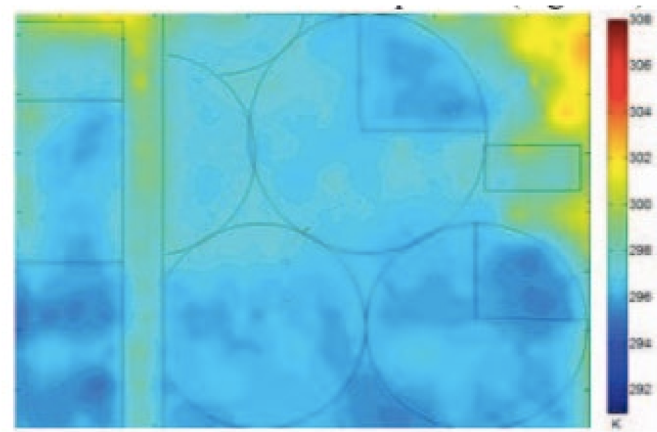

(a)

Lake and river bathymetry from UAS

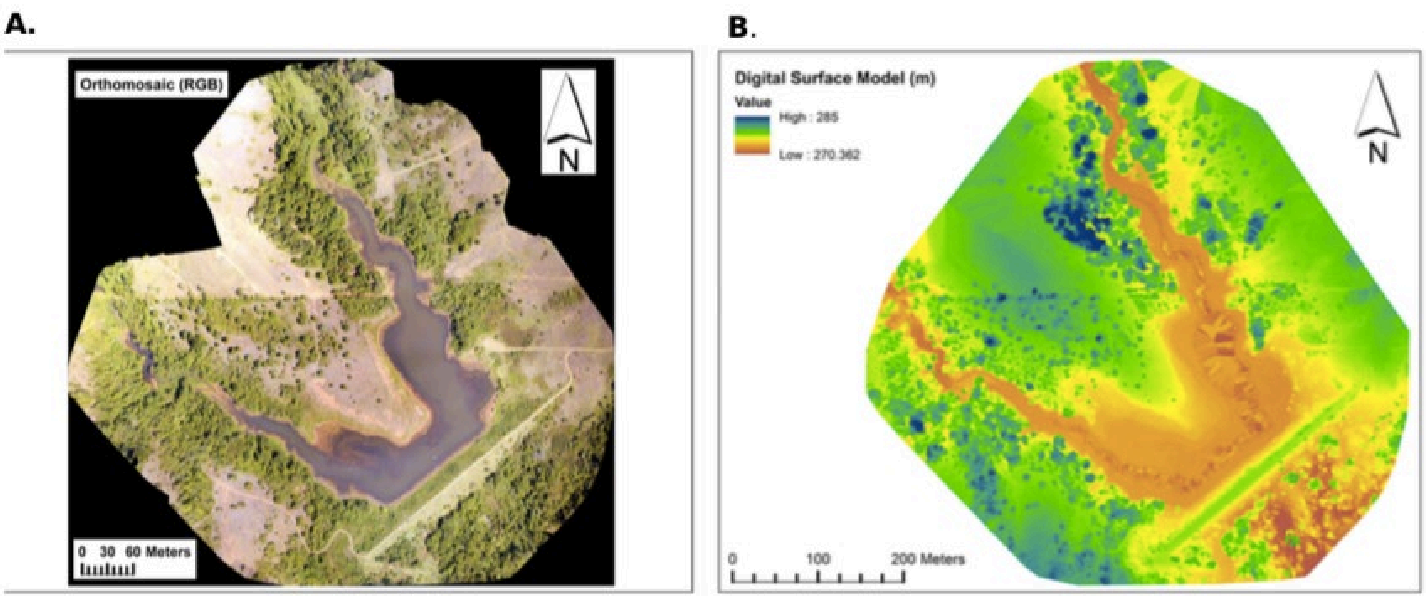

Figure 3. Pix4D software outputs: Orthomosaic and corresponding Digital Elevation Model (DEM)

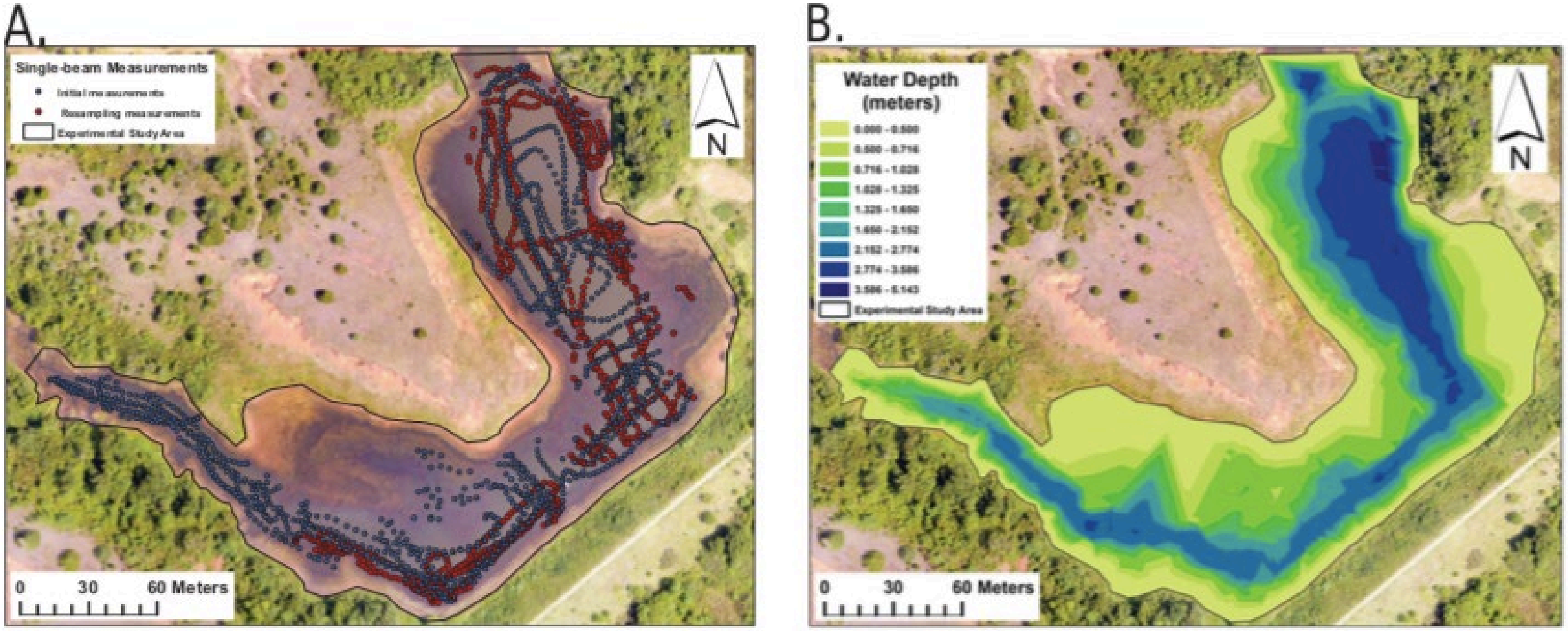

Figure 6. Bathymetry of Finn Creek 21 Reservoir using the single-beam echosounder. (a) Cumulative sampling points taken with the single-beam echosounder during August of 2017. (b) Bathymetric mapping built with the single-beam echosounder is shown.

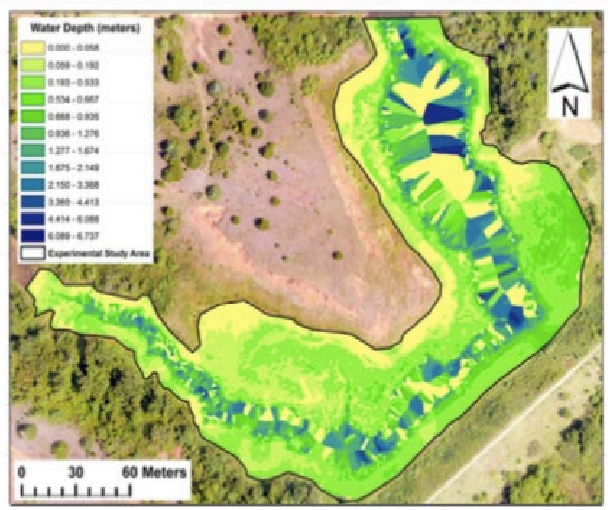

Figure 8. Bathymetry of Finn Creek 21 Reservoir using UAS-SfM technique taken during August of 2017.